# Development and application of an algorithm for detecting *Phaeocystis globosa* blooms in the Case 2 Southern North Sea waters

ROSA ASTORECA[1]*, VÉRONIQUE ROUSSEAU[1], KEVIN RUDDICK[2], CÉCILE KNECHCIAK[1], BARBARA VAN MOL[2], JEAN-YVES PARENT[1] AND CHRISTIANE LANCELOT[1]

[1]ECOLOGIE DES SYSTÈMES AQUATIQUES (ESA), FACULTÉ DES SCIENCES, UNIVERSITÉ LIBRE DE BRUXELLES, CAMPUS PLAINE, CP 221, BOULEVARD DU TRIOMPHE, B-1050 BRUSSELS, BELGIUM AND [a]MANAGEMENT UNIT OF THE NORTH SEA MATHEMATICAL MODELS (MUMM), ROYAL BELGIAN INSTITUTE FOR NATURAL SCIENCES, 100 GULLEDELLE, B-1200 BRUSSELS, BELGIUM

*CORRESPONDING AUTHOR: rastorec@ulb.ac.be

*While mapping algal blooms from space is now well-established, mapping undesirable algal blooms in eutrophicated coastal waters raises further challenge in detecting individual phytoplankton species. In this paper, an algorithm is developed and tested for detecting Phaeocystis globosa blooms in the Southern North Sea. For this purpose, we first measured the light absorption properties of two phytoplankton groups, P. globosa and diatoms, in laboratory-controlled experiments. The main spectral difference between both groups was observed at 467 nm due to the absorption of the pigment chlorophyll c3 only present in P. globosa, suggesting that the absorption at 467 nm can be used to detect this alga in the field. A Phaeocystis-detection algorithm is proposed to retrieve chlorophyll c3 using either total absorption or water-leaving reflectance field data. Application of this algorithm to absorption and reflectance data from Phaeocystis-dominated natural communities shows positive results. Comparison with pigment concentrations and cell counts suggests that the algorithm can flag the presence of P. globosa and provide quantitative information above a chlorophyll c3 threshold of 0.3 mg m$^{-3}$ equivalent to a P. globosa cell density of $3 \times 10^6$ cells L$^{-1}$. Finally, the possibility of extrapolating this information to remote sensing reflectance data in these turbid waters is evaluated.*

## INTRODUCTION

In recent years, several attempts have been made to identify phytoplankton functional groups using ocean colour data. These studies serve different purposes such as (i) harmful algal bloom detection (Millie *et al.*, 1997; Kahru and Mitchell, 1998; Staehr and Cullen, 2003), (ii) accurate retrieval of satellite-derived chlorophyll *a* concentrations in waters with different dominating phytoplankton populations (Sathyendranath *et al.*, 2004) or (iii) mapping the distribution of phytoplankton groups (i.e. diatoms) at a global scale (Alvain *et al.*, 2005).

Discrimination and identification between phytoplankton groups is based on their inherent optical properties, namely light absorption and backscattering (Stuart *et al.*, 2000; Vaillancourt *et al.*, 2004). The inter-species differences in these optical properties can be retrieved from remote sensing data provided they are distinct enough to alter the absorption/reflectance spectra at certain wavelengths and do not vary significantly with the physiological state of the phytoplankton. The light absorption characteristics of phytoplankton groups depend on the pigment composition (Hoepffner

and Sathyendranath, 1991) and on packaging (Morel and Bricaud, 1981). Pigment composition, and specifically the proportion of auxiliary pigments such as carotenoids relative to the total chlorophyll *a* content, varies with light or nutrient regimes (Johnsen *et al.*, 1994; Henriksen *et al.*, 2002; Staehr *et al.*, 2002).

Certain bloom forming species with specific optical signatures have already been identified from remote sensing. With the notable exception of coccolithophores which can be detected from their very strong scattering (Smyth *et al.*, 2002), taxa-specific algorithms are generally based on detecting the absorption of one or more pigments which are characteristic of the target taxa. For example, the unique combination of absorption features in the green (565 nm) caused by phycobilipigments of cyanobacteria, e.g. *Trichodesmium*, forms the basis of an algorithm for the detection of this genus (Subramaniam *et al.*, 1999). The ultraviolet absorption characteristics of red-tide forming dinoflagellates have been used by Kahru and Mitchell (Kahru and Mitchell, 1998) to differentiate them from other species. An algorithm for mapping of cyanobacteria in inland waters was developed by Simis *et al.* (Simis *et al.*, 2005), who detected phycocyanin based on red absorption (620 nm).

The prymnesiophyte *Phaeocystis globosa*, referred hereafter as *Phaeocystis*, blooms each spring in the Southern Bight of the North Sea stimulated by nitrate enrichment (Lancelot, 1995; Lancelot *et al.*, 1998). This species forms large ungrazed colonies (up to 3 mm diameter) that accumulate in the water and create, under windy conditions, thick layers of foul-smelling foam on beaches, making it undesirable (Lancelot *et al.*, 1987; Lancelot, 1995). At that time of the year, *Phaeocystis* and diatoms form the bulk phytoplankton community in the Belgian coastal zone (Rousseau, 2000; Muylaert *et al.*, 2006) and together can reach high levels of chlorophyll *a* detectable from space (Peters *et al.*, 2005). The relative contribution of diatom and *Phaeocystis* to the spring bloom varies between years with most years being dominated by *Phaeocystis* (Breton *et al.*, 2006).

Satellite imagery provides useful information on concentrations of chlorophyll *a* and can be used as a tool for mapping the magnitude and the geographical extent of blooms in this area. However, the bulk chlorophyll *a* information is not sufficient to identify whether a bloom consists of the undesirable *Phaeocystis*. Recently, Lubac *et al.* (Lubac *et al.*, 2008) proposed multispectral and hyperspectral approaches to detect *Phaeocystis* based on two reflectance ratios and the position of the maxima and minima of second derivative analysis of reflectance spectra, respectively. These methods are essentially qualitative and are discussed in more detail later.

The objective of this study is to identify an optical feature which could be used to discriminate between diatoms and *Phaeocystis* on the basis of reflectance data and hence to develop an algorithm for the detection of *Phaeocystis* in turbid coastal waters. As a first step, the differences in the absorption signature of cultured *Phaeocystis* and diatoms representative of the Belgian coastal zone are analysed under different light conditions. The differences in the water-leaving reflectance spectra are then analysed for samples dominated either by diatoms or *Phaeocystis*. Finally, an algorithm is developed and validated to detect the presence and quantify *Phaeocystis* in Southern North Sea waters and the possibility of detecting *Phaeocystis* from space is assessed.

# METHOD

## Cultures

Pure strains of the diatoms *Thalassiosira rotula* and *Ditylum brightwellii* were obtained from the Plymouth Culture Collection. The *P. globosa* strain BCZ05 was isolated from the central Belgian Coastal Zone. Inoculates were grown in nutrient replete conditions in 0.2 μm filtered seawater enriched with F20 medium in Nalgene polycarbonate flasks placed over stir plates in a culture room at 8–10°C under a 12 h:12 h light:dark cycle. Silicate was added to the diatom cultures. Two different light intensities were applied to each species: 100 (HL) and 10 (LL) μmol quanta $m^{-2} s^{-1}$ (Philips Master TL-D 30W/865).

## Field samples

Sampling was carried out in Belgian and adjacent coastal waters during 7 campaigns covering spring, summer and late summer from 2004 to 2007 aboard the RV Belgica. The area is characterized by high biomass phytoplankton blooms that, combined with sediment resuspension (Fettweis and Van Den Eynde, 2003) and dissolved material from riverine origin, result in an optically complex type of water (Astoreca *et al.*, 2006). Sampling stations are reported in Fig. 1. At all stations, water-leaving reflectance was measured and a 20 L seawater sample was taken at the surface for the measurement of particulate, phytoplankton and coloured dissolved organic matter (CDOM) light absorption, high performance liquid chromatography (HPLC) pigments and phytoplankton community composition. Filtration was performed immediately after sampling. Filters were kept in liquid nitrogen less than 1 week and then stored at −80°C until analysis. Both cultures and field samples were sampled for light absorption, pigments and phytoplankton counts.
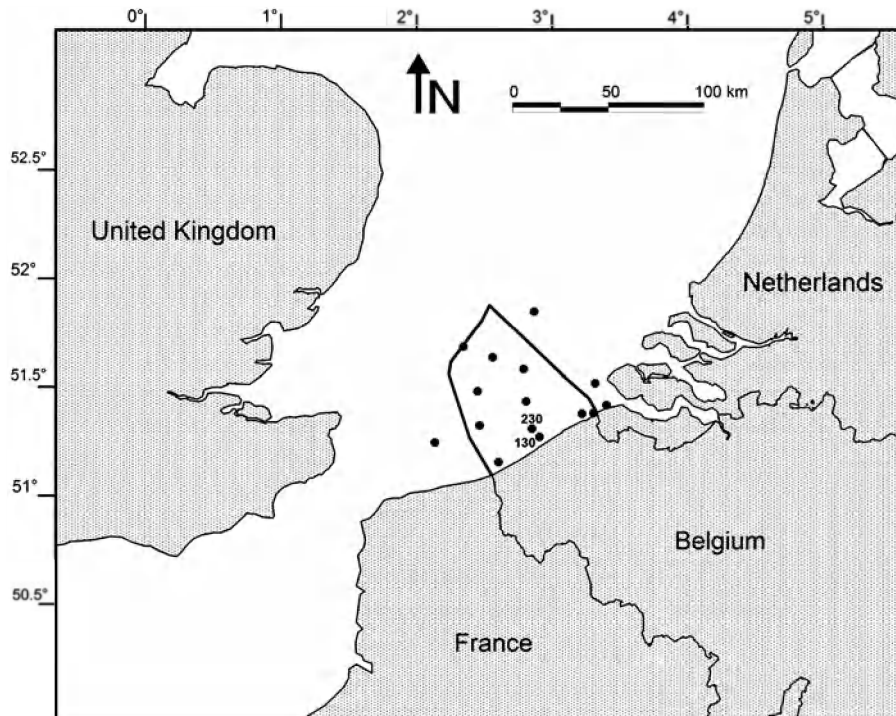
**Fig. 1.** Sampling stations in the Belgian Coastal Zone and adjacent waters in the Southern North Sea. Borders of the Belgian Coastal Zone are indicated as bold lines.

## Water-leaving reflectance measurements

Water-leaving radiance reflectance $\rho_w$, was calculated from simultaneous above-water measurements of downwelling irradiance $E_d^{0+}$, upwelling radiance $L_{sea}^{0+}$ and sky radiance $L_{sky}^{0+}$, using three TriOS-RAMSES hyperspectral spectroradiometers mounted on a steel frame at the prow of the RV Belgica with zenith angles of the sea- and sky-viewing radiance sensors of $40°$:

$$\rho_w = \frac{\pi\left(L_{sea}^{0+} - \rho_{sky}L_{sky}^{0+}\right)}{E_d^{0+}} \quad (1)$$

where $\rho_{sky}$ is the reflection coefficient for the wave-roughened air-water interface. This corresponds to "Method 1" of the NASA protocols (Mueller *et al.*, 2000). More information on this system and data processing can be found in Ruddick *et al.* (Ruddick *et al.* 2006).

## Light absorption determination

*Phytoplankton, particle and total absorption measurements*
Seawater was filtered onto 25 mm glass fibre filters (Whatman GF/F). The absorbance spectra of particles $OD_{part}(\lambda)$ retained on each filter was determined

following the transmittance−reflectance method (Tassan and Ferrari, 1995). The transmittance and reflectance of each filter were measured between 400 and 750 nm with a UVIKON 930 dual beam spectrophotometer equipped with a 6 cm-integrating sphere for the 2004−2006 samples and with a Perkin Elmer Lambda 650 spectrophotometer equipped with a 15 cm-integrating sphere for the 2007 samples. The absorbance spectrum of non-algal particles retained on the filter $OD_{NAP}(\lambda)$ was measured after particle bleaching with NaOCl (0.13% active chlorine) following Ferrari and Tassan (Ferrari and Tassan, 1999). Pathlength amplification was corrected using an algorithm which has been validated for several phytoplankton species and non-algal particles (Tassan and Ferrari, 1998). Absorbance values at each wavelength were converted into absorption coefficients by:

$$a_{part/NAP}(\lambda) = \frac{2.303^* OD_{part/NAP}(\lambda)}{X} \quad (2)$$

where $X$ is the ratio of filtered volume to the filter clearance area.

The absorption spectra $a_{part/NAP}(\lambda)$ were then corrected for scattering in the near infrared by subtracting an average over 748−752 nm from all the measured

spectra (Babin *et al.*, 2003). The $a_{NAP}(\lambda)$ spectra were corrected by fitting an exponential function to the data between 400 and 750 nm (Babin *et al.*, 2003).

The phytoplankton absorption coefficient $a_{ph}$ $(m^{-1})$ was obtained from

$$a_{ph}(\lambda) = a_{part}(\lambda) - a_{NAP}(\lambda) \qquad (3)$$

Absorption spectra of $a_{ph}$ were normalized at 675 nm in order to remove the variations associated with chlorophyll *a* and to highlight the differences in the blue-green part of the spectrum.

### CDOM absorption measurements

Some 100 mL of seawater were filtered through a 0.2 μm Nuclepore polycarbonate membrane, prefiltered with Milli-Q water. This filtrate was used to rinse both a clean amber bottle and the filtration flask and was then discarded. A second volume was filtered and kept in the bottle at 4°C. Absorbance of the filtered water was measured in a UVIKON 930 dual beam spectrophotometer using a 10 cm quartz cuvette (Tilstone *et al.*, 2002). Absorbance values $(OD_{CDOM})$ at each wavelength were converted into absorption coefficients $a_{CDOM}$ using:

$$a_{CDOM}(\lambda) = \frac{2.303^* OD_{CDOM}(\lambda)}{l} \qquad (4)$$

where $l$ (m) is the length of the cuvette.

A baseline correction was applied to the $a_{CDOM}$ spectra by subtracting an average over 683–687 nm from all the spectral values (Babin *et al.*, 2003).

The total absorption coefficient $a_t$ was obtained from

$$a_t(\lambda) = a_{part}(\lambda) + a_{CDOM}(\lambda) + a_w(\lambda) \qquad (5)$$

where $a_w$ is the absorption of pure water obtained from Buiteveld *et al.* (Buiteveld *et al.* 1994).

### Pigment determination

Subsamples were filtered onto 25 mm glass Whatman GF/F filters for HPLC chlorophyll *a* and pigment determination. Filters were kept at $-80°C$ until analysis. HPLC determination was carried out following Wright *et al.* (Wright *et al.*, 1991). Cut filters were sonicated in centrifuge tubes with 2 mL of 100% cold acetone for 30 s and then left at 4°C for 2 h before centrifugation. Pigment extracts were analysed using a Waters HPLC system (Waters 600 Controller, Waters 717 Autosampler and Waters 996 Photodiode Array

Detector) and a reverse-phase Waters Spherisorb 5 μm ODS2 column. The linear solvent gradient included solvent A (80:20 methanol: 0.5 M ammonium acetate), solvent B (90:10 acetonitrile:water) and solvent C (100% ethyl acetate). Pigments were detected by absorption at 436 nm and identified based on comparison of retention time and spectra with standards (International Agency for ^{14}C determination, Denmark). The main pigments identified were the light harvesting pigments (LHP): chlorophyll *c3* (chl *c3*), chlorophyll *c1+2* (chl *c1+2*), chlorophyll *a* (chl *a*) and fucoxanthin (fuco), and the photo-protective carotenoids (PPC): diadinoxanthin (diadino), diatoxanthin (diato) and betacaroten (beta-car).

### Phytoplankton enumeration and biomass

Some 10–50 mL of phytoplankton sub-sample, preserved with 1% lugol-glutaraldehyde solution and stored at 4°C in the dark, were analysed under inverted microscopy (Leitz Fluovert, Germany) according to the Utermöhl method. At least 400 cells were enumerated in each sample. Magnification was chosen according to phytoplankton size: 40X or 100X for *Phaeocystis* colonies, and 100X or 200X for diatoms. *Phaeocystis* colony cell density was determined based on colony volume measurements (Rousseau *et al.*, 1990). Diatom carbon biomass was calculated on the basis of cell concentration and specific biometry using the size-dependant density relationship recommended by Menden-Deuer and Lessard (Menden-Deuer and Lessard, 2000). The carbon biomass of *Phaeocystis* colonies was estimated by biovolume measurement (Rousseau *et al.*, 1990). *Phaeocystis*- and diatom-dominance in a sample was defined on the basis of a biomass contribution of >70%.

### Data treatment and statistics

The entire dataset comprises a total of 85 measurements. From the 7 sampling campaigns only those in bloom condition reflected by healthy *Phaeocystis* colonies were considered. The final dataset for the development and validation of the algorithm consists then of 31 samples.

The second derivative of each absorption spectrum was computed with the software Peakfit 4.12 to identify and resolve the position of the absorption maxima attributable to photosynthetic pigments. The second derivative analysis identifies portions of the absorption spectra that have the greatest curvature. In general, local minima in the second derivative correspond to spectral regions with enhanced absorption.

The Mann–Whitney $U$ statistic was used to test the differences between two groups of samples at different wavelengths.

## RESULTS

### Identification of a unique spectral absorption feature in *Phaeocystis*

Figure 2A–C compares the normalized phytoplankton absorption $a_{ph}$ spectra for the two diatoms and *Phaeocystis* each grown at two light levels. Differences in the magnitude of the phytoplankton absorption $a_{ph}$ spectra are observed for both phytoplankton groups

when comparing growth conditions. The two diatom species show an enhanced absorption between 400 and 510 nm at HL and between 510 and 650 nm at LL (Fig. 2A and B). *Phaeocystis* shows enhanced absorption between 400 and 490 nm at HL (Fig. 2C). No significant differences in magnitude and shape of the spectra were found when comparing phosphorus limited and phosphorous replete conditions for both diatoms and *Phaeocystis* (data not shown).

The spectral shape of $a_{ph}$ is similar between both diatoms and light conditions but different from that of *Phaeocystis* (Fig. 2A–C). The spectral second derivative analysis of the two diatom spectra identifies seven major absorption maxima for both HL and LL conditions, i.e. at 412, 437, 465, 500, 587, 637 and 675 nm (Fig. 2D
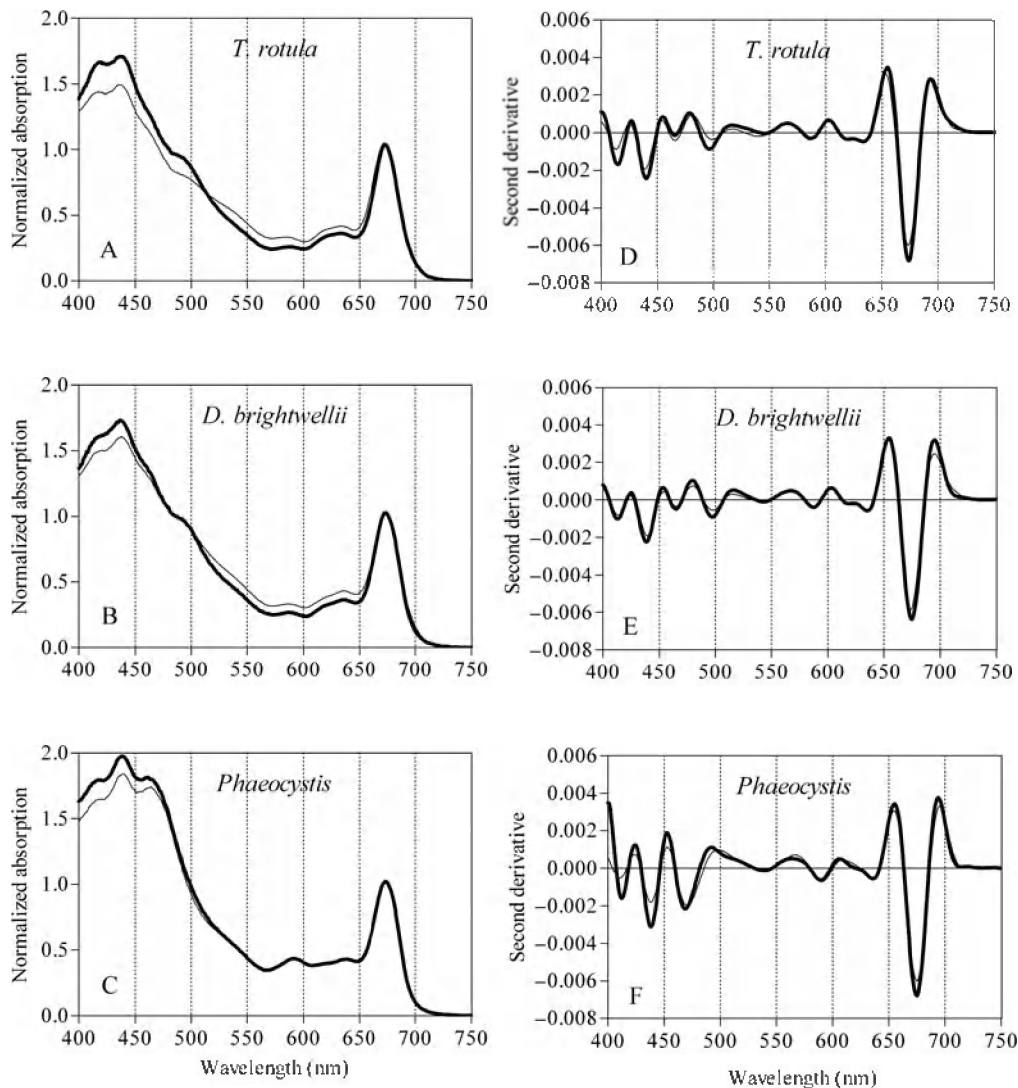


**Fig. 2.** Phytoplankton absorption $a_{ph}$ spectra normalized to 675 nm for the diatoms *T. rotula* (**A**), *D. brightwellii* (**B**) and the prymnesiophyte *Phaeocystis* (**C**) for HL and LL conditions. Second derivative analysis calculated from the absorption spectra for the diatoms *T. rotula* (**D**), *D. brightwellii* (**E**) and the prymnesiophyte *Phaeocystis* (**F**). HL (thick line): 100 μmol quanta m$^{-2}$ s$^{-1}$, LL (thin line): 10 μmol quanta m$^{-2}$ s$^{-1}$.

*Table I: Mann−Whitney U-test showing the variability in the normalized phytoplankton absorption for the two light conditions within each species (intra-species), between diatoms, and between diatoms and Phaeocystis (inter-species)*

| Species | Conditions | | Wavelengths (nm) | | | | | |
|---|---|---|---|---|---|---|---|---|
| | | | 412 | 437 | 467 | 500 | 588 | 637 |
| *T. rotula* | HL−LL | U | 6.0 | 6.0 | 6.0 | 6.0 | 0 | 0 |
| | | p | 0.08 | 0.08 | 0.08 | 0.08 | 0.08 | 0.08 |
| *D. brightwellii* | HL−LL | U | 6.0 | 6.0 | 6.0 | 3.0 | 1.0 | 0 |
| | | p | 0.08 | 0.08 | 0.08 | 1 | 0.24 | 0.08 |
| *Phaeocystis* | HL−LL | U | 9.0 | 9.0 | 5.0 | – | 0 | 0 |
| | | p | 0.05 | 0.05 | 0.83 | – | 0.05 | 0.05 |
| *T. rotula-D. brightwellii* | | U | 10.0 | 8.0 | 0.5 | 1.5 | 10.5 | 8.5 |
| | | p | 0.60 | 0.35 | 0.01* | 0.02* | 0.68 | 0.40 |
| Diatoms-*Phaeocystis* | | U | 4.0 | 3.0 | 0 | – | 3.0 | 12.5 |
| | | p | 0.005* | 0.003* | 0.001** | – | 0.003* | 0.06 |

*$P < 0.05$, level of significance.
**$P < 0.001$, level of significance.

and E). The second derivative spectrum of *Phaeocystis* identifies only six major absorption maxima, i.e. at 412, 438, 467, 588, 636 and 675 nm, the maximum at 500 nm being absent in *Phaeocystis* (Fig. 2F).

Normalized phytoplankton absorption at the maxima wavelengths identified by the second derivative analysis was used to characterize the intra- and inter-species variability of absorption spectra (Table I). No significant intra-species variability of phytoplankton absorption resulting from HL and LL growth conditions was observed either for the two diatoms or for *Phaeocystis* (Table I). Comparison between both diatoms shows significant differences at 467 and 500 nm ($P < 0.01$ and $P < 0.02$ respectively; Table I).

Inter-species differences between diatoms and *Phaeocystis* are much more significant at all wavelengths except 637 nm, with the highest significant difference at 467 nm ($P < 0.001$; Table I).

The absorption coefficient of phytoplankton results from the absorption of all pigments present in a sample (Hoepffner and Sathyendranath, 1991) and is affected by the pigment packaging (Morel and Bricaud, 1981). The concentrations per cell for the main pigments of both diatoms and *Phaeocystis*, measured during the different experiments, are shown in Table II. Comparison between the two groups shows that they share the same pigment composition except for chl *c3* which is only present in *Phaeocystis*.

The effects of light conditions on pigments suggest that diatoms and *Phaeocystis* increase the synthesis of LHP at LL. The PPC remain stable in *T. rotula* and *Phaeocystis* but increase in *D. brightwellii* at LL.

The contribution of the different pigments to the observed maxima of the phytoplankton absorption spectrum (Fig.2A−C) was estimated on the basis of

*Table II: Pigment concentrations normalized to cell number (pg cell⁻¹) for the different growth conditions of the species*

| Pigments | *T. rotula* | | *D. brightwellii* | | *Phaeocystis* | |
|---|---|---|---|---|---|---|
| | HL | LL | HL | LL | HL | LL |
| chl *c3* | 0 | 0 | 0 | 0 | 0.65 | 0.64 |
| chl *c1+2* | 0.21 | 0.83 | 3.78 | 17.82 | 0.13 | 0.16 |
| chl *a* | 1.30 | 4.92 | 33.59 | 68.96 | 1.76 | 1.78 |
| fuco | 0.36 | 0.90 | 10.58 | 23.27 | 0.35 | 0.53 |
| LHP | 1.86 | 6.66 | 47.95 | 110.06 | 2.89 | 3.10 |
| diadino | 0.10 | 0.10 | 5.17 | 4.59 | 0.08 | 0.07 |
| diato | 0.06 | 0.02 | 0.62 | 1.55 | 0.06 | 0.04 |
| Beta-car | 0.05 | 0.09 | 0.84 | 2.50 | 0.002 | 0.02 |
| PPC | 0.21 | 0.21 | 6.64 | 8.63 | 0.14 | 0.13 |

HL: 100 µmol quanta m⁻² s⁻¹, LL: 10 µmol quanta m⁻² s⁻¹.
LHP: light-harvesting pigments, PPC: photo-protective carotenoids.

a correlation analysis performed between the absorption at maxima identified by the second derivative analysis (Fig. 2D−F) and the absolute pigment concentrations (Table III). The wavelengths of absorption maxima of *in vivo* pigments were extracted from Hoepffner and Sathyendranath (Hoepffner and Sathyendranath, 1991) and Johnsen *et al.* (Johnsen *et al.*, 1994) for comparison with our wavelengths identified by second derivative analysis. Results show significant contributions of the different pigments at the following wavelengths: chl *a* at 412 nm and at 437 nm, chl *c3* at 467 nm, fuco and beta-car at 500 nm, chl *c3* and chl *a* at 588 m, and chl *a* at 637 nm and at 675 nm (Table III).

The low significance of the intra-species variability of phytoplankton absorption $a_{ph}$ spectra for both diatoms and *Phaeocystis* compared to the higher differences observed between diatoms and *Phaeocystis* allows the use of $a_{ph}$ spectra averaged between light conditions to

*Table III: Correlations between phytoplankton absorption $a_{ph}$ ($m^{-1}$) at main wavelengths from the second derivative analysis and absolute pigment concentrations (mg m$^{-3}$)*

| Wavelength (nm) | chl *c1 + 2* | chl *c3* | fuco | diadino | diato | beta-car | chl *a* |
|---|---|---|---|---|---|---|---|
| 412 | | | | | | | 0.85* |
| 437 | | | 0.62 | 0.53 | 0.05 | 0.05 | 0.85* |
| 467 | 0.17 | 0.87* | 0.57 | | | | |
| 500 | | | 0.92* | 0.81 | 0.90 | 0.95* | |
| 588 | 0.22 | 0.86* | | | | | 0.83* |
| 637 | 0.40 | 0.74 | | | | | 0.92* |
| 675 | | | | | | | 0.93* |

Pigments related to these wavelengths were extracted from literature (Hoepffner and Sathyendranath, 1991; Johnsen *et al.*, 1994).
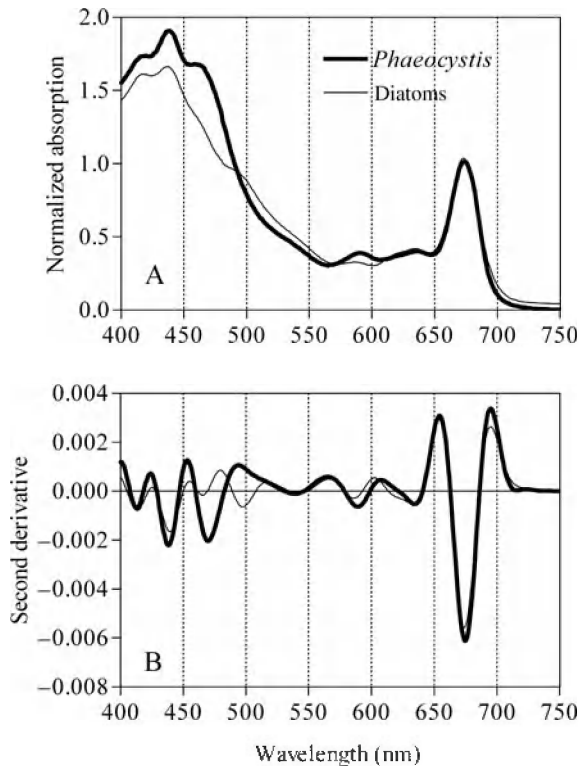*$P < 0.05$, level of significance.



**Fig. 4.** Measured chl *c3* (mg m$^{-3}$) as a function of *Phaeocystis* cell number ($10^6$ L$^{-1}$) for field Belgian Coastal Zone data. Regression line for this relationship is shown.

587 nm (Fig. 3A). The second derivative analysis (Fig. 3B) shows clearly that the minimum observed at 467 nm is only present in *Phaeocystis* and is much more pronounced than the slight minimum observed at 465 nm for diatoms. At 500 nm, the second derivative of $a_{ph}$ for diatoms shows a local minimum that is not present in *Phaeocystis*. Statistical analysis suggests 467 nm as the wavelength at which the difference between diatoms and *Phaeocystis* is the most pronounced (Table I) and thus, could serve for the discrimination between these groups. *Phaeocystis* absorption at 467 nm corresponds to the presence of chl *c3* (Table III). The use of chl *c3* as a marker of *Phaeocystis* cells is further supported by the good correlation (Pearson $r = 0.95$, $P < 0.0001$, $n = 31$) between chl *c3* concentration and *Phaeocystis* cell density for data collected in Belgian waters during *Phaeocystis* blooms (Fig. 4).

## Development of a *Phaeocystis*-detection algorithm based on retrieval of chl *c3*

The *Phaeocystis* phytoplankton absorption $a_{ph}$ at 467 nm is then used for the development of a *Phaeocystis* detection algorithm which can be used with both total absorption $a_t$ and water-leaving reflectance $\rho_w$ data. This algorithm is based on a "baseline" concept where two blue bands are chosen on either side of the chl *c3* absorption band, the third band $\lambda_{c3} = 467$ nm.

### *Absorption algorithm*

The basic assumption of the algorithm is that $a_t$ at $\lambda_{c3}$ in the absence of chl *c3*, denoted as $a_{t-c3}$, can be sufficiently well-approximated by an exponential interpolation of $a_t$ between $\lambda_1$ and $\lambda_2$:

$$a_{t-c3}(\lambda_{c3}) = a_t(\lambda_1)^{[1-w]} * a_t(\lambda_2)^w \qquad (6)$$



**Fig. 3.** Average phytoplankton absorption $a_{ph}$ spectra of diatoms and of *Phaeocystis* normalized to 675 nm from cultures at different light growth conditions (**A**) and second derivative analysis (**B**).

highlight the differences between both groups (Fig. 3). The main differences in spectral shape observed between the mean $a_{ph}$ spectra of diatoms and of *Phaeocystis* are found between 450 and 520 nm and at
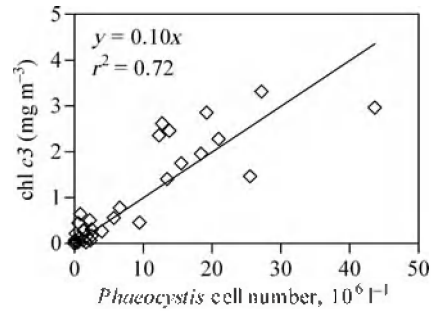
where the interpolation weighting is given by:

$$w = \frac{\lambda_{c3} - \lambda_1}{\lambda_2 - \lambda_1} \qquad (7)$$

This exponential interpolation is preferred over a linear one because it will fit better the absorption spectrum in the presence of particulate or dissolved yellow substance.

Then the deviation from the baseline that can be attributed to chl $c3$ at $\lambda_{c3}$ ($a_{c3}$), namely the "extra chl $c3$ absorption", can be calculated from:

$$a_{c3}(\lambda_{c3}) = a_t(\lambda_{c3}) - a_t(\lambda_1)^{[1-w]} * a_t(\lambda_2)^w \qquad (8)$$

The wavelengths $\lambda_1$ and $\lambda_2$ are chosen at 450 and 480 nm, respectively, because they are located at the extremes of the chl $c3$ absorption maximum (Fig. 3) and thus are not affected by chl $c3$ absorption.

The algorithm (8), given in its absorption version, can be used directly as a three-band algorithm for retrieving $a_{c3}$ from *in situ* measurements of total absorption $a_t(\lambda_1)$, $a_t(\lambda_2)$ and $a_t(\lambda_{c3})$, noting that these measurements must include all absorbing components, i.e.

phytoplankton, non-algal particles, CDOM and pure water itself.

The algorithm is demonstrated in Fig. 5A which shows two total absorption $a_t$ spectra measured for *Phaeocystis*-dominated and diatom-dominated samples. One spectrum was measured at station 130 on the 10 May 2004 during a bloom of *Phaeocystis* (chl $a = 43.9$ mg m$^{-3}$, chl $c3 = 2.97$ mg m$^{-3}$, $a_{CDOM}(442) = 0.36$ m$^{-1}$). The other spectrum was recorded at station 230 the 30 June 2005 during a diatom dominated condition (chl $a = 7.44$ mg m$^{-3}$, chl $c3 = 0.00$ mg m$^{-3}$, $a_{CDOM}(442) = 0.27$ m$^{-1}$). The principle of the baseline algorithm is shown in Fig. 5B which shows an enlargement of Fig. 5A between 440 and 500 nm. For the diatom-dominated sample (June 2005), the measured total absorption $a_t$ coincides with the baseline at 467 nm, indicating no impact of the pigment chl $c3$. In contrast, for the *Phaeocystis*-dominated sample (May 2004), the measured $a_t$ is noticeably higher than the baseline at 467 nm. This difference between the baseline and the measured $a_t$, albeit small (equivalent to an absorption coefficient difference of about 0.1 m$^{-1}$), is attributed to chl $c3$ absorption.

### Reflectance algorithm

For use with satellite data, this algorithm must be expressed with water-leaving reflectance $\rho_w$ as input.
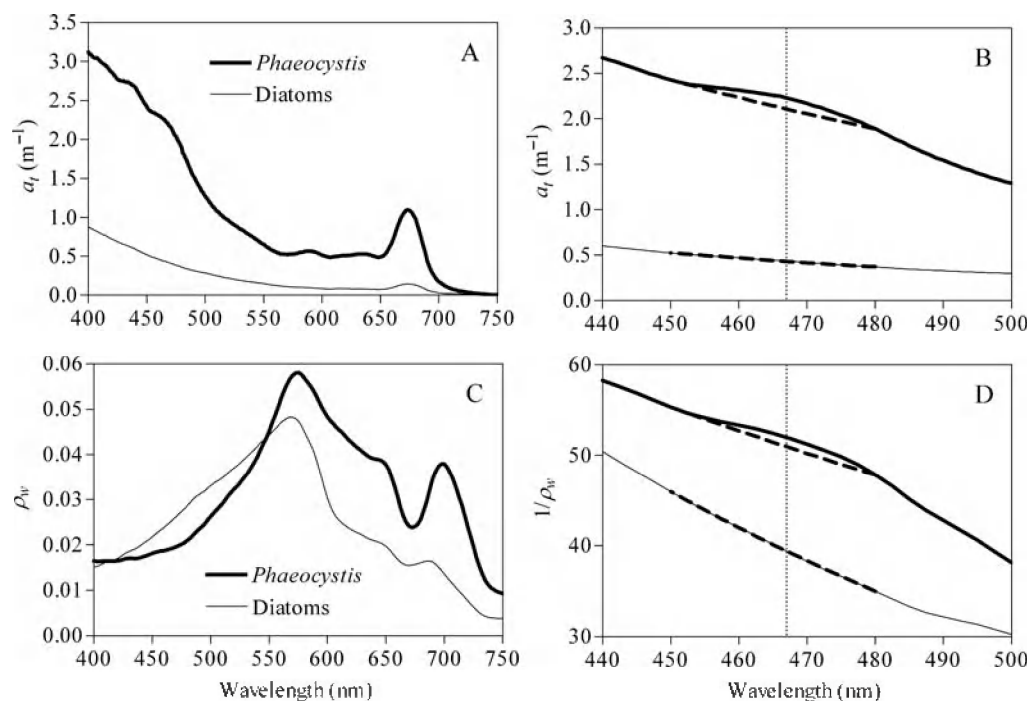


**Fig. 5.** Total absorption $a_t$ (m$^{-1}$) spectra (**A**) and water-leaving reflectance $\rho_w$ (**C**) measured at sea for *Phaeocystis*-dominated (10 May 2004) and diatom-dominated (30 June 2005) samples. Enlargement of the region 440–500 nm to show the principle of the algorithm based on $a_t$ (**B**) and reciprocal of water-leaving reflectance $1/\rho_w$ for the spectra shown in (C) with enlargement of the region 440–500 nm (**D**). The baselines obtained by exponential interpolation between 450 and 480 nm are superimposed as bold dotted lines (B and D). The 467 nm feature is shown as a vertical dotted line.

Since $\rho_w$ depends on both total absorption $a_t$, and total backscatter $b_b$, it is necessary to use reflectance ratios to remove dependence on backscatter and isolate the absorption-related signal. This is achieved by using an extra fourth band $\lambda_{NIR}$, chosen in the near infrared (NIR) and supposing that (i) $a_t$ ratios can be approximated by the reciprocal of the corresponding $\rho_w$ ratio, i.e. $a_t(\lambda)/a_t(\lambda_{NIR}) \approx \rho_w(\lambda_{NIR})/\rho_w(\lambda)$ and 2) $a_t$ can be approximated by the pure water absorption coefficient in the NIR, $a_t(\lambda_{NIR}) \approx a_w(\lambda_{NIR})$ giving:

$$a_t(\lambda_i) \approx a_w(\lambda_{NIR}) * \frac{(\rho_w(\lambda_{NIR}))}{(\rho_w(\lambda_i))} \quad \text{for } i = 1, 2, c3 \quad (9)$$

In certain circumstances this approximation may be less accurate. For example, in Case 1 waters or in Case 2 waters with significantly non-white particles or for extremely turbid waters there may be significant spectral variation of the product $\rho_w(\lambda) * a_t(\lambda)$. Such cases are beyond the scope of the present study but may still be amenable to retrieval of chl $c3$ by appropriate modification of equation (9) or redesign of this component of the model.

Substituting from equation (9) into (8) gives the algorithm for retrieval of chl $c3$ from reflectance data:

$$a_{c3}(\lambda_{c3}) = \left( \frac{1}{\rho_w(\lambda_{c3})} \right. $$
$$\left. - \frac{1}{\rho_w(\lambda_1)^{(1-w)}} * \frac{1}{\rho_w(\lambda_2)^w} \right) * a_w(\lambda_{NIR}) * \rho_w(\lambda_{NIR})$$
$$(10)$$

Here the NIR band $\lambda_{NIR} = 700$ nm is chosen using data for $a_w(700) = 0.57 \text{ m}^{-1}$ reported by Buiteveld *et al.* (Buiteveld *et al.*, 1994).

Thus, the chl $c3$ absorption at $\lambda_{c3}$ given by $a_{c3}(\lambda_{c3})$ can be estimated from the reflectance measurements at four bands $\rho_w(\lambda_1)$, $\rho_w(\lambda_2)$, $\rho_w(\lambda_{c3})$ and $\rho_w(\lambda_{NIR})$.

To illustrate this algorithm, Fig. 5C shows the two $\rho_w$ spectra measured during the *Phaeocystis*-dominated and diatom-dominated bloom conditions as in Fig. 5A. The $\rho_w$ version of this algorithm is shown in Fig. 5D, which corresponds to the reciprocal of the $\rho_w$ spectra from Fig. 5C. For the diatom-dominated sample (June 2005), the measured $\rho_w$ reciprocal is slightly below the baseline at 467 nm, indicating a negligible impact of the pigment chl $c3$. In contrast, the measured reciprocal of $\rho_w$ of the *Phaeocystis*-dominated sample (May 2004) is noticeably higher than the baseline at 467 nm. This difference between the baseline and the measured $\rho_w$, albeit small

(equivalent to a $\rho_w$ difference of only 0.0004), is attributed to chl $c3$ absorption. The algorithm (10) uses this difference, normalized by the product of $\rho_w$ and pure water absorption at a NIR wavelength, to estimate the extra absorption from chl $c3$. The chl $c3$ absorption retrieved from $\rho_w$ is estimated as $0.022 \text{ m}^{-1}$ and $-0.0001 \text{ m}^{-1}$ for the *Phaeocystis* (May) and diatom (June) spectra, respectively. In this case, there is a clear distinction between the two taxa on the basis of $\rho_w$ spectra at the 467 nm chl $c3$ absorption peak.

## Validation of the chl *c3* retrieval algorithm

Figure 6A and B compares the chl $c3$ absorption retrieved from total absorption and from reflectance data with measured chl $c3$ concentrations. The regression performed using total absorption data input ($r^2 = 0.72$, $P < 0.0001$, $n = 31$) gives much better results than that performed using reflectance data input ($r^2 = 0.56$, $P < 0.0001$, $n = 31$). The relation between chl $c3$ and *Phaeocystis* cell number shown in Fig. 4 is then used for converting chl $c3$ concentration into *Phaeocystis* biomass (Fig. 6C and D) to allow the quantification of the bloom. The results of the regressions give a higher regression coefficient for chl $c3$ absorption retrieved from total absorption $a_t$ with *Phaeocystis* cell number ($r^2 = 0.94$, $P < 0.0001$, $n = 31$) than for chl $c3$ absorption retrieved from $\rho_w$ and *Phaeocystis* cell number ($r^2 = 0.57$, $P < 0.0001$, $n = 31$).

## DISCUSSION

### Pigment composition and absorption of *Phaeocystis* and diatoms

In this paper, an algorithm based on the absorption of chl $c3$ at 467 nm is proposed to detect *Phaeocystis* in field samples. The extent to which chl $c3$ is specific of *Phaeocystis* is discussed here based on the absorption characteristics of *Phaeocystis* and diatoms.

The characteristic $a_{ph}$ spectral shape shown by *Phaeocystis* with main peaks at 412, 440 and 467 nm is also found for both *P. pouchetii* (Stuart *et al.*, 2000) and for *P. antarctica* (Moisan and Mitchell, 1999) suggesting that these are characteristic of the family Phaeocystaceae. The diatoms investigated show an enhanced $a_{ph}$ at 412, 440 and 500 nm, as already reported for the diatoms *Thalassiosira* spp., *Chaetoceros* spp. and *Skeletonema costatum* (Sathyendranath *et al.*, 1987; Johnsen *et al.*, 1994; Stuart *et al.*, 2000; Stramski *et al.*, 2002). The $a_{ph}$ signature of diatoms and *Phaeocystis* results from their specific pigment composition. The pigment composition obtained for our
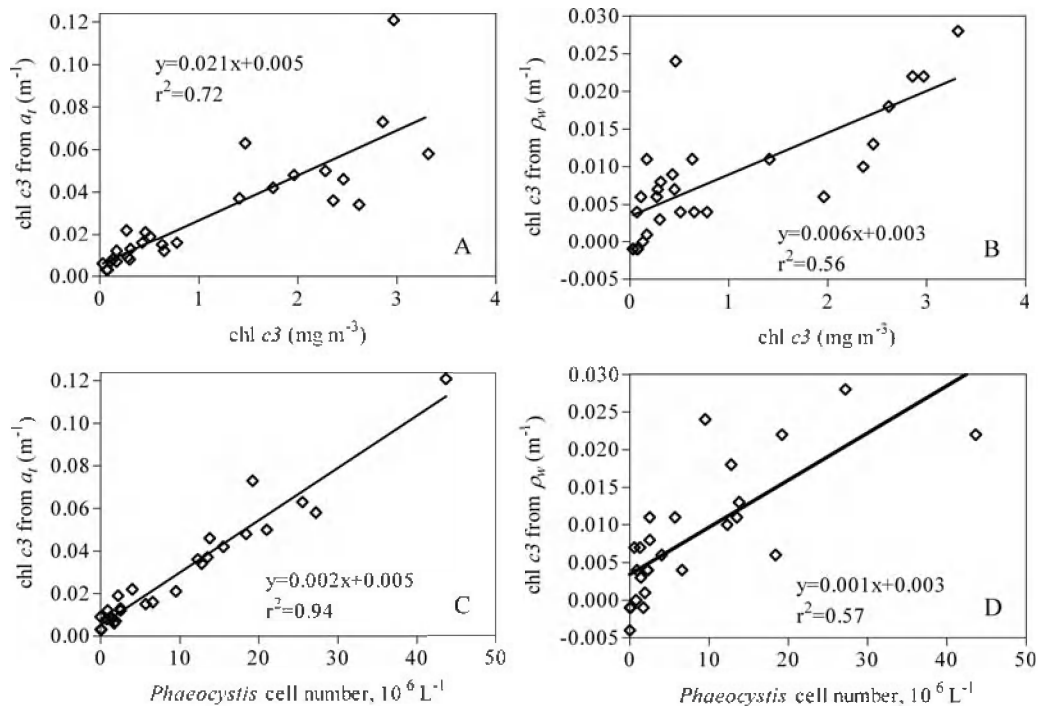
**Fig. 6.** (**A**) Chl *c3* retrieval from total absorption $a_t$ data using the algorithm developed in equation (8) and (**B**) chl *c3* retrieval from water-leaving reflectance $\rho_w$ data using the algorithm developed in equation (10), as a function of field chl *c3* concentration. (**C**) Chl *c3* retrieval from total absorption $a_t$ data using the algorithm developed in equation (8) and (**D**) chl *c3* retrieval from water-leaving reflectance $\rho_w$ data using the algorithm developed in equation (10), as a function of *Phaeocystis* cell number.

*P. globosa* strain (Table II) is similar to that found for another strain of the same species (Zapata *et al.*, 2004) and also for *P. pouchetii* (Llewellyn and Gibb, 2000), and for *P. antarctica* (Moisan and Mitchell, 1999). The reported pigment composition for *Phaeocystis* includes chl *a*, chl *c1 + 2*, chl *c3*, 19'butanoyloxyfucoxanthin, 19'hexanoyloxyfucoxanthin, fuco, diadino, diato and beta-car. In our *Phaeocystis* cultures, however, no 19'butanoyloxyfucoxanthin or 19'hexanoyloxyfucoxanthin were detected. The absence of these two carotenoids has already been reported for *P. globosa* blooms in Belgian waters (Antajan *et al.*, 2004; Muylaert *et al.*, 2006) and in the English Channel (Breton, 2000) and constitutes a significant difference between high-latitude and North Sea *Phaeocystis* species. Our results for pigment composition of diatoms which include chl *a*, chl *c1 + 2*, fuco, diadino, diato and beta-car agree with that reported for 10 species of diatoms of different size (Llewellyn and Gibb, 2000). The highest pigment to chl *a* contribution is made by fuco in diatoms and chl *c3* followed by fuco in *Phaeocystis* (Table II). The latter result is similar to that of Moisan and Mitchell (Moisan and Mitchell, 1999) who found that chlorophylls *c* are the major contributors in prymnesiophytes. As shown by pigment compositions, the main difference between *Phaeocystis* and diatoms is the presence of chl *c3* in *Phaeocystis* which absorbs at 467 nm and differs from chl *c1+2* present in diatoms and *Phaeocystis* which absorbs at 465 nm.

The significant regression between retrieved chl *c3* absorption and *Phaeocystis* cell number suggests that the detection of chl *c3* indicative of a *Phaeocystis* bloom is possible when the phytoplankton community is dominated by *Phaeocystis*, i.e. during the spring bloom. Chl *c3* is a marker of *Phaeocystis* species (Claustre *et al.*, 1990; Vaulot *et al.*, 1994; Breton *et al.*, 2000; Antajan *et al.*, 2004), but its presence has been reported in most of the prymnesiophytes (Jeffrey and Wright, 1994; Zapata *et al.*, 2004) and in some diatoms such as *Rhizosolenia setigera* or *Thalassionema nitzchioïdes* (Stauber and Jeffrey, 1988: Llewellyn and Gibb, 2000). In the Belgian waters, however, *Phaeocystis* is the dominant prymnesiophyte and the proportion of chl *c3* containing diatoms is negligible during the year (Rousseau, 2000). Therefore, chl *c3* has been found to be a good marker for *Phaeocystis* in Belgian waters, as previously found for the English Channel (Breton, 2000). However, the *Phaeocystis* cellular content of chl *c3* (0.10 pg chl *c3* cell$^{-1}$) estimated from our field data, i.e. the slope of the regression line in Fig. 4, is higher than those previously reported for the English Channel (0.06 pg chl *c3* cell$^{-1}$; Breton *et al.*, 2000) and for Belgian waters (0.05−0.07 pg chl *c3* cell$^{-1}$; Antajan *et al.*, 2004).

## Estimation of the uncertainty in the retrieval of chl *c3* from absorption and water-leaving reflectance spectra

The algorithm developed in this work, defined by equations (8) and (10), can be used to flag the presence of chl *c3* concentrations and to quantify *Phaeocystis* blooms in the field. The algorithm results can, however, be subject to interference from other water components, namely non-algal particles and CDOM, both of them usually referred to as yellow substance (YS), which are present in variable amounts in Belgian waters (Astoreca *et al.*, 2006). For example, in the multispectral approach proposed by Lubac *et al.* (Lubac *et al.*, 2008) to detect *Phaeocystis* blooms using current ocean colour sensors in the Eastern English Channel, two remote sensing reflectance ratios ($R_{rs}(490)/R_{rs}(510)$ and $R_{rs}(442.5)/R_{rs}(490)$) were found to be successful. However, a sensitivity analysis showed that the behaviour of the first ratio is highly sensitive to the relative contribution of CDOM and to the phytoplankton assemblage composition (Lubac *et al.*, 2008).

To investigate whether our algorithm is affected by YS (non-algal particle+CDOM absorption), the algorithm was applied to absorption of non-chl *c3* containing phytoplankton on the one hand and of YS on the other hand (Fig. 7). This corresponds to the error, expressed in absorption, caused by the baseline approximation for samples with no chl *c3*. The absorption of non-chl *c3* containing phytoplankton ($n = 29$) and of YS ($n = 85$) were taken from field measurements comprised in the entire database. The non-chl *c3* containing phytoplankton includes different proportions of diatoms. The YS absorption at 467 nm varies from 0.08 to 2.16 m$^{-1}$ and the spectral slope varies from 0.010 to 0.018 nm$^{-1}$. As a reference, the variation in the optical constituents of these coastal waters is illustrated in Fig. 8 with phytoplankton absorption contributing from 14 to 73%; NAP from 2 to 67% and CDOM from 7 to 81% to total absorption.
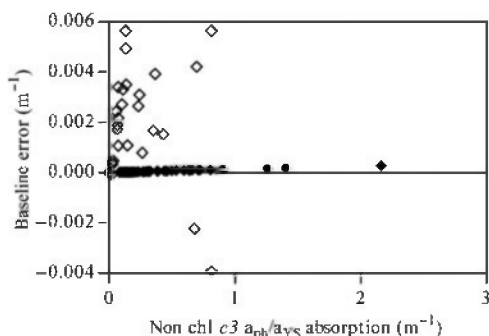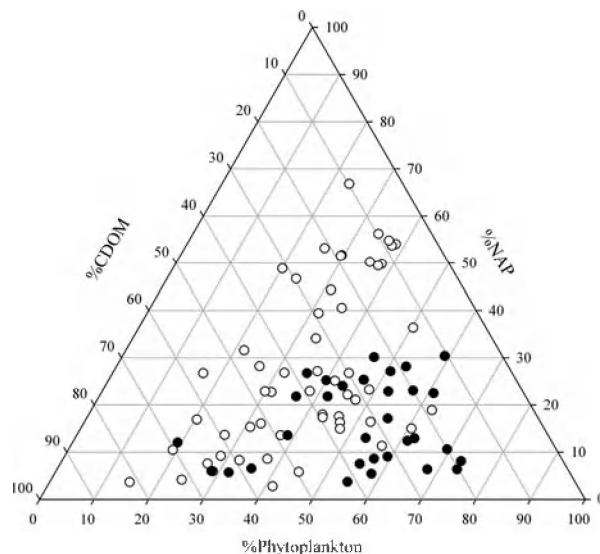


**Fig. 8.** Ternary plot illustrating the relative contribution of CDOM, phytoplankton and NAP to total absorption at 467 nm, for all samples in this study, including the chl *c3* containing (filled circles) and the non-chl *c3* containing samples (open circles). The relative contribution of a given absorption component for a given sample can be read on the corresponding axis, where the component label is positioned at the middle of the scale for that component.

Remarkably, because of the exponential baseline approach, the YS baseline error is nearly zero, showing that the algorithm is not affected by YS absorption and thus can be used in turbid Case 2 waters, e.g. Southern Bight of the North Sea. The baseline error for non-chl *c3* phytoplankton has a maximum value of 0.006 m$^{-1}$ meaning that below this value the algorithm is not able to detect extra chl *c3* from *Phaeocystis*. This probably explains the scattering observed at low chl *c3* concentrations in the relationship between retrieved extra chl *c3* either from $a_t$ or $\rho_w$ with measured chl *c3* (Fig. 6). Thus, the limit from which the *Phaeocystis* bloom can be detected is 0.3 mg chl *c3* m$^{-3}$ equivalent to $3 \times 10^6$ cells L$^{-1}$. Coincidentally, this value is close to the reference abundance of *Phaeocystis* cells from which the disturbance from a well-balanced ecosystem in coastal *Phaeocystis*-dominated ecosystems could be scaled (i.e. $4 \times 10^6$ cells L$^{-1}$, Lancelot *et al.*, 2008) suggesting that the ocean colour could be used for detecting undesirable blooms of *Phaeocystis* in Belgian coastal waters provided all other sources of uncertainty can be sufficiently controlled.

## Applicability and limitations of the chl *c3* retrieval

Since the magnitude of the chl *c3* absorption is small, it is unlikely that accurate quantitative retrieval of this



**Fig. 7.** Baseline error results when applying the algorithm to non-chl *c3* phytoplankton (open diamonds) and to YS data (filled diamonds).

pigment will be possible from remote sensing in the way that chl $a$ is now routinely retrieved. However, the results show that the detection of *Phaeocystis* blooms would be possible for *Phaeocystis* cell concentrations higher than $3 \times 10^6$ cells $L^{-1}$ (Fig. 6C and D). Below this threshold, the large uncertainty precludes retrieval of accurate *Phaeocystis* cell density. At this stage, the algorithm described here may be used as a *Phaeocystis* flag and could supplement chl $a$ imagery by providing basic information on the presence of undesirable *Phaeocystis*. It is likely that this flag will be subject to a detection limit for chl $c3$ absorption retrieved from $\rho_w$ of $0.006 \, \mathrm{m}^{-1}$ since only the higher chl $c3$ absorption conditions will noticeably affect the $\rho_w$ spectrum. Thanks to a careful design via a baseline technique which removes most of the interference from non-phytoplankton absorption the present algorithm is likely to provide reliable detection of chl $c3$ absorption (or concentration) even in the presence of non-algal particle and CDOM absorption. Finally, the present version of the algorithm is not suitable for high $\rho_w$ (e.g. above 0.06) since the assumption $a_t(\lambda)/a_t(\lambda_{\mathrm{NIR}}) \approx \rho_w(\lambda_{\mathrm{NIR}})/\rho_w(\lambda)$ must then be modified to account for the non-linear increase of $\rho_w$ with backscatter.

## Is remote sensing of *Phaeocystis* from space feasible?

In the previous sections, various issues have been identified which add uncertainties when transforming an algorithm based on phytoplankton absorption to algorithms based on total absorption and hence on reciprocal water-leaving reflectance. The further problem of atmospheric correction errors will affect the performance of satellite algorithms for *Phaeocystis* detection. The use of a baseline technique operating over a short wavelength range will ensure that atmospheric correction errors relating to the spectrally-correlated errors typical of imperfect aerosol estimation or Rayleigh-aerosol coupling will have minimal impact on algorithm performance. The absence of significant wavelength-specific gaseous absorption features near the wavelengths considered (450, 467 and 480 nm) is also a positive feature. However, the very small perturbations on the water-leaving reflectance spectrum that need to be detected will impose a constraint on the radiometric performance of the sensor and spectrally uncorrelated errors at the level of 0.0001 or above arising from atmospheric correction or sensor calibration are likely to cause interference in attempts to use chl $c3$ absorption as a way of detecting *Phaeocystis* blooms. The present study provides a realistic perspective for taxon-specific detection and thus guides the design of future

sensors regarding wavelength requirements for chl $c3$ detection (450 nm, 467 nm and 480 nm, or preferably hyperspectral) and radiometric accuracy required.

## REFERENCES

Alvain, S., Moulin, C., Dandonneau, Y. *et al.* (2005) Remote sensing of phytoplankton groups in case 1 waters from global SeaWiFS imagery. *Deep-Sea Res. I*, **52**, 1989–2004.

Antajan, E., Chrétiennot-Dinet, M. -J., Leblanc, C. *et al.* (2004) 19′-hexanoyloxyfucoxanthin may not be the appropriate pigment to trace occurrence and fate of *Phaeocystis*: the case of *P. globosa* in Belgian coastal waters. *J. Sea Res.*, **52**, 165–177.

Astoreca, R., Ruddick, K., Van Mol, B. *et al.* (2006) Variability of the Inherent and Apparent Optical Properties in a highly turbid coastal area: Impact for the calibration of Remote Sensing algorithms. *EARSeL eProceedings*, **5**, 1–17.

Babin, M., Stramski, D., Ferrari, G. M. *et al.* (2003) Variations in the light absorption coefficients of phytoplankton, nonalgal particles, and dissolved organic matter in coastal waters around Europe. *J. Geophys. Res.*, **108**, 3211. doi:10.1029/2001JC000882.

Breton, E. (2000) Qualité du pool nutritif et nutrition des copépodes pélagiques en Manche orientale. Thèse de doctorat, Université du Littoral-Cote d'Opale, 281pp.

Breton, E., Brunet, C., Sautour, B. *et al.* (2000) Annual variations of phytoplankton biomass in the Eastern English Channel: comparison by pigment signatures and microscopic counts. *J. Plankton Res.*, **22**, 1423–1440.

Breton, E., Rousseau, V., Parent, J.-Y. *et al.* (2006) Hydroclimatic modulation of diatom/*Phaeocystis* blooms in nutrient-enriched Belgian coastal waters (North Sea). *Limnol. Oceanogr.*, **51**, 1401–1409.

Buiteveld, H., Hakvoort, J. M. H. and Donze, M. (1994) The optical properties of pure water. In Jaffe, J. S.(ed.), *Proceedings of Ocean Optics XII, SPIE*, pp. 174–183.

Claustre, H. A. P. S., Williams, R., Marty, J.-C. *et al.* (1990) A biochemical investigation of a *Phaeocystis* sp. bloom in the Irish Sea. *J. Mar. Biol. Assoc. UK*, **70**, 197–207.

Ferrari, G. and Tassan, S. (1999) A method using chemical oxidation to remove light absorption by phytoplankton pigments. *J. Phycol.*, **35**, 1090–1098.

Fettweis, M. and Van Den Eynde, D. (2003) The mud deposits and the high turbidity in the Belgian-Dutch coastal zone, Southern Bight of the North Sea. *Cont. Shelf Res.*, **23**, 669–691.

Henriksen, P., Riemann, B., Kaas, H. *et al.* (2002) Effects of nutrient-limitation and irradiance on marine phytoplankton pigments. *J. Plankton Res.*, **24**, 835–858.

Hoepffner, N. and Sathyendranath, S. (1991) Effect of pigment composition on absorption properties of phytoplankton. *Mar. Ecol. Prog. Ser.*, **73**, 11–23.

Jeffrey, S. and Wright, S. (1994) Photosynthetic pigments in the Haptophyta. In Green, J. C. and Leadbeater, B. S. C. (eds), *The Haptophyta Algae*. Clarendon Press, Oxford, pp. 111–132.

Johnsen, G., Samset, O., Granskog, L. *et al.* (1994) *In vivo* absorption characteristics in 10 classes of bloom-forming phytoplankton: taxonomic characteristics and responses to photoadaptation by means of discriminant and HPLC analysis. *Mar. Ecol. Prog. Ser.*, **105**, 149–157.

Kahru, M. and Mitchell, B. G. (1998) Spectral reflectance and absorption of a massive red tide off Southern California. *J. Geophys. Res.*, **103**, 601–621.

Lancelot, C. (1995) The mucilage phenomenon in the continental coastal waters of the North Sea. *Sci. Total Environ.*, **165**, 83–102.

Lancelot, C., Billen, G., Sournia, A. *et al.* (1987) Phaeocystis blooms and nutrient enrichment in the continental coastal zones of the North Sea. *Ambio*, **16**, 38–46.

Lancelot, C., Keller, M., Rousseau, V. *et al.* (1998) Autoecology of the marine haptophyte *Phaeocystis* sp. In Anderson, D. A., Cembella, A. M. and Hallegraef, G. (eds), *NATO Advanced Workshop on the physiological ecology of Harmful Algal Blooms*. NATO-ASI Series 41 Series G Ecological Science, pp. 209–224.

Lancelot, C., Rousseau, V. and Gypens, N. (2008) Ecologically-based indicators for *Phaeocystis* disturbance in eutrophied Belgian coastal waters (Southern North Sea) based on field observations and ecological modeling. *J. Sea Res.* doi:10.1016/j.seares.2008.05.010. In press.

Llewellyn, C. A. and Gibb, S. W. (2000) Intra-class variability in the carbon, pigment and biomineral content of prymnesiophytes and diatoms. *Mar. Ecol. Prog. Ser.*, **193**, 33–44.

Lubac, B., Loisel, H., Guiselin, N. *et al.* (2008) Hyperspectral and multispectral ocean color inversions to detect *Phaeocystis globosa* blooms in coastal waters. *J. Geophys. Res.*, **113**, C06026. doi:10.1029/2007JC004451.

Menden-Deuer, S. and Lessard, E. J. (2000) Carbon to volume relationships for dinoflagellates, diatoms, and other protist plankton. *Limnol. Oceanogr.*, **45**, 569–579.

Millie, D. F., Schofield, O. M., Kirkpatrick, G. J. *et al.* (1997) Detection of harmful algal blooms using photopigments and absorption signatures: a case study of the Florida red tide dinoflagellate *Gymnodinium breve*. *Limnol. Oceanogr.*, **42**, 1240–1251.

Moisan, T. A. and Mitchell, B. G. (1999) Photophysiological acclimation of *Phaeocystis antarctica* Karsten under light limitation. *Limnol. Oceanogr.*, **44**, 247–258.

Morel, A. and Bricaud, A. (1981) Theoretical results concerning light absorption in a discrete medium, and applications to specific absorption of phytoplankton. *Deep-Sea Res.*, **28**, 1375–1393.

Mueller, J., Davis, C., Arnone, R. *et al.* (2000) Above-water radiance and remote sensing reflectance measurements and analysis protocols. *Ocean Optics protocols for satellite ocean color sensor validation. Revision 2.* NASA, Greenbelt, Maryland, pp. 98–107.

Muylaert, K., Gonzalez, R., Franck, M. *et al.* (2006) Spatial variation in phytoplankton dynamics in the Belgian coastal zone of the North Sea studied by microscopy, HPLC-CHEMTAX and underway fluorescence recordings. *J. Sea Res.*, **55**, 253–265.

Peters, S. W. M., Eleveld, M. A., Pasterkamp, R. *et al.* (2005) *Atlas of Chlorophyll-a concentration for the North Sea based on MERIS imagery of 2003.* Vrije Universiteit Amsterdam, The Netherlands.

Rousseau, V. (2000) *Dynamics of Phaeocystis and diatom blooms in the eutrophicated coastal waters of the Southern Bight of the North Sea.* PhD Thesis. Université Libre de Bruxelles, Bruxelles, 205 pp.

Rousseau, V., Mathot, S. and Lancelot, C. (1990) Calculating carbon biomass of *Phaeocystis* sp. from microscopic observations. *Mar. Biol.*, **107**, 305–314.

Ruddick, K., De Cauwer, V., Park, Y. *et al.* (2006) Seaborne measurements of near infrared water-leaving reflectance: The similarity spectrum for turbid waters. *Limnol. Oceanogr.*, **51**, 1167–1179.

Sathyendranath, S., Lazzara, L. and Prieur, L. (1987) Variations in the spectral values of specific absorption of phytoplankton. *Limnol. Oceanogr.*, **32**, 403–415.

Sathyendranath, S., Watts, L., Devred, E. *et al.* (2004) Discrimination of diatoms from other phytoplankton using ocean-colour data. *Mar. Ecol. Prog. Ser.*, **272**, 59–68.

Simis, S. G. H., Peters, S. W. M. and Gons, H. J. (2005) Remote sensing of the cyanobacterial pigment phycocyanin in turbid inland water. *Limnol. Oceanogr.*, **50**, 237–245.

Smyth, T. J., Moore, G. F., Groom, S. B. *et al.* (2002) Optical modeling and measurements of a coccolithophore bloom. *Appl. Opt.*, **41**, 7679–7688.

Staehr, P. A. and Cullen, J. J. (2003) Detection of *Karenia mikimotoi* by spectral absorption signatures. *J. Plankton Res.*, **25**, 1237–1249.

Staehr, P. A., Henriksen, P. and Markager, S. (2002) Photoacclimation of four marine phytoplankton species to irradiance and nutrient availability. *Mar. Ecol. Prog. Ser.*, **238**, 47–59.

Stauber, J. L. and Jeffrey, S. W. (1988) Photosynthetic pigments in fifty-one species of marine diatoms. *J. Phycol.*, **24**, 158–172.

Stramski, D., Sciandra, A. and Claustre, H. (2002) Effects of temperature, nitrogen, and light limitation on the optical properties of the marine diatom *Thalassiosira pseudonana*. *Limnol. Oceanogr.*, **47**, 392–403.

Stuart, V., Sathyendranath, S., Head, E. J. *et al.* (2000) Bio-optical characteristics of diatom and prymnesiophyte populations in the Labrador Sea. *Mar. Ecol. Prog. Ser.*, **201**, 91–106.

Subramaniam, A., Carpenter, E. J., Karentz, D. *et al.* (1999) Bio-optical properties of the marine diazotrophic cyanobacteria *Trichodesmium* spp. I. Absorption and photosynthetic action spectra. *Limnol. Oceanogr.*, **44**, 608–617.

Tassan, S. and Ferrari, G. (1995) An alternative approach to absorption measurements of aquatic particles retained on filters. *Limnol. Oceanogr.*, **40**, 1358–1368.

Tassan, S. and Ferrari, G. (1998) Measurement of light absorption by aquatic particles retained on filters: determination of the optical

pathlength amplification by the 'transmittance-reflectance' method. *J. Plankton Res.*, **20**, 1699–1709.

Tilstone, G., Moore, G. F., Sorensen, K. *et al.* (2002) *REVAMP, Regional Validation of MERIS Chlorophyll products in North Sea coastal water, REVAMP protocols document.* EU, EVG1-CT-2001-00049, 77 pp.

Vaillancourt, R. D., Brown, C. W., Guillard, R. R. *et al.* (2004) Light backscattering properties of marine phytoplankton: relationships to cell size, chemical composition and taxonomy. *J. Plankton Res.*, **26**, 191–212.

Vaulot, D., Birrien, J. B., Marie, D. *et al.* (1994) Morphology, ploidy, pigment composition, and genome size of cultured strains of *Phaeocystis* (Prymnesiophyceae). *J. Phycol.*, **30**, 1022–1035.

Wright, S., Jeffrey, S., Mantoura, R. *et al.* (1991) An improved HPLC method for the analysis of chlorophylls and carotenoids from marine phytoplankton. *Mar. Ecol. Prog. Ser.*, **77**, 183–196.

Zapata, M., Jeffrey, S. W., Wright, S. W. *et al.* (2004) Photosynthetic pigments in 37 species (65 strains) of Haptophyta: implications for oceanography and chemotaxonomy. *Mar. Ecol. Prog. Ser.*, **270**, 83–102.